Computers and Electronics in Agriculture 178 (2020) 105799

Contents lists available at ScienceDirect

Computers and Electronics in Agriculture

journal homepage: www.elsevier.com/locate/compag

Development of a grass measurement optimisation tool to efficiently measure herbage mass on grazed pastures

D.J. Murphy [a,b], B. O' Brien [a], M.D. Murphy [b,*]

[a] Teagasc, Animal & Grassland Research and Innovation Centre, Moorepark, Fermoy, Co., Cork, Ireland
[b] Department of Process, Energy and Transport Engineering, Cork Institute of Technology, Cork, Ireland

A R T I C L E I N F O

Keywords:
Grass measurement
Grass utilisation
Measurement protocol
Traveling salesman problem
Monte Carlo simulation
Grassland optimisation

A B S T R A C T

Accurate and efficient estimation of herbage mass is essential for optimising grass utilisation and increasing profit for pasture farming. There is no definitive sampling protocol for grass measurement on Irish pastures. This paper presents the Grass Measurement Optimisation Tool (GMOT), designed to generate measurement protocols that optimise for time and accuracy. The GMOT was designed in the form of a decision support tool that generates interactive paddock maps that guide the farmer on how to optimally measure their pastures in a random stratified manner based on GPS co-ordinates, resulting in accurate non-biased estimations of mean herbage mass. Rising plate meter (RPM) measurements and reference herbage cuts were performed on trial plots and grazed paddocks over three years. Measurement routes were optimised using a genetic algorithm based on a traveling salesman problem. Actual survey error was estimated in terms of relative prediction error using Monte Carlo simulations that combined measurement and calibration error distributions for the RPM. Cost benefit analysis was conducted to evaluate the feasibility of using the GMOT on Irish grasslands. Actual error for the RPM decreased from 37% to 26% as measurement rates increased from 1 to 8 ha^{-1} and reductions in error were negligible (<1%) as measurements increased from 8 to 32 ha^{-1}. Calibration error was the largest source of error (25.9%) compared to measurement error (8%). Optimal measurement value was achieved by performing 8 measures ha^{-1} and further increasing the measurement rate resulted in diminishing returns. The GMOT is compatible with a range of pasture measurement technologies.

1. Introduction

Accurately predicting fresh grass quantity, in terms of herbage mass (HM) (kg DM ha^{-1}), is essential in allocating the correct quantity of grass to the herd on a daily basis and in maintaining high levels of utilisation (Delaby et al., 1998; Dillon, 2006). Beukes et al., (2019) reported that a 15% increase in farm profitability could be achieved by carrying out regular pasture measurements. Dillon (2011) and Hanrahan et al., (2018) estimated that every additional tonne of HM utilised by grazing is worth between €160 – €278. Traditionally HM was measured by cutting and weighing grass samples, however non-destructive and less laborious means of estimating HM such as the rising plate meter (RPM) have become more popular with farmers (Ferraro et al., 2012; Lile et al., 2001; Thomson, 1983). More recent developments have led to the increased use of online decision support tools (DST) in conjunction with grass measurement devices, such as the RPM, to assist with the HM calculation and allocation processes. PastureBase Ireland (PBI) is a DST that is capable of uploading RPM compressed sward height (CSH) data to predict herbage yields both in terms of HM, by means of an equation developed by Delaby et al., (1998), and growth rates using previously recorded data (Hanrahan et al., 2017). Pasturebase is similar to other DSTs developed in Europe (Delaby et al., 2015; Zom and Holshof, 2011). Moreover, scope for a holistic grass management DST that incorporates more precise and efficient grass measurement technologies and practices has been identified (Murphy et al., 2019).

Several studies have highlighted two of the main sources of error for the RPM as being measurement protocol and HM prediction error (Earle and Mc Gowan, 1979; Klootwijk et al., 2019a; Lile et al., 2001; Sanderson et al., 2001). Protocol error relates to the number of measures and the measurement route taken within a pasture. Studies have shown that HM can vary between 15 – 60% within pastures as a result of selective grazing and dung pats, making it difficult to accurately estimate and allocate on a regular basis (Barthram et al., 2005; Hirata, 2000; Jordan

* Corresponding author.
E-mail address: MichaelD.Murphy@cit.ie (M.D. Murphy).

https://doi.org/10.1016/j.compag.2020.105799
Received 9 June 2020; Received in revised form 18 September 2020; Accepted 19 September 2020
Available online 1 October 2020

et al., 2003; Klootwijk et al., 2019a; Nakagami, 2016). Murphy et al. (2020a) recorded average HM variance of 36% within Irish perennial rye grass (*Lolium perenne L.*) (PRG) dairy paddocks.

There is no definitive measurement protocol for the RPM to accurately predict mean HM and account for spatial variation within pastures. Measurements are typically carried out 30 – 50 times in a 'Zig Zag' pattern or along transects of a paddock (Sanderson et al., 2001; Thomson et al., 1997), which leaves scope for operator error and bias. Haydock & Shaw (1975) stated that increasing sampling area and resolution will in turn increase measurement precision, but this further increases sampling time, effort and cost. Moreover, increasing measurement rate does not guarantee proportional increases in precision and a number of studies have outlined that the relationship between measurement rate and accuracy is in accordance with the law of diminishing returns (Hutchinson et al., 2016; Murphy et al., 2020a; O' Sullivan et al., 1987). Reducing measurement time and effort is paramount, not only in saving time and cost for farmers but also to encourage more farmers to measure grass on a regular basis.

Scope for a universal grass measurement protocol has long been identified (Haydock and Shaw, 1975; Murphy et al., 2018; Thomson et al., 1997). Hutchinson et al., (2016) developed sampling guidelines to determine the number of RPM measurements required based upon the farmers desired level of accuracy and effort. However these guidelines required the operator to visually asses pasture variation and select measurement locations, leaving considerable scope for bias. Studies have suggested the use of random stratified sampling (RSS) to best predict HM within pastures, however this is difficult to implement at farm level due to constraints on time and resources (Cayley and Bird, 1996; Hutchinson et al., 2016; Mannetje, 2000). Employing RSS involves dividing a paddock into several equally sized strata and then assigning an equal number of samples randomly within each stratum. This allows for an even and non-biased distribution of samples within the paddock (Stevens and Olsen, 2004; Webster and Lark, 2012). Murphy et al., 2020a developed a relationship between RPM measurement rate and average CSH estimation error based on RSS. One issue with RSS is that it can increase measurement labour, as the operator has to walk to each pre-determined random measurement location instead of walking the fastest route through the paddock. To minimise the distance walked and ultimately the labour requirement when carrying out a grass measurement survey, a route optimisation procedure must be employed. This is similar to a common route optimisation problem often referred to as the travelling salesman problem (TSP), based on the analogy of a salesman that needs to travel to number of cities and return home in the shortest period of time. Solving a TSP can be extremely computationally expensive as all possible route combinations need to be calculated. Alternatively, a genetic algorithm (GA) can be employed to estimate the most optimum route in a reasonable time frame. A GA mimics evolutionary processes in nature such as natural selection to estimate the most optimum route (Abdoun and Abouchabaka, 2012; Haupt and Haupt, 2004). Recent studies have applied TSP approaches to solve agricultural route optimisation problems in areas such as automated targeted weed control and field operational logistics (Stray et al., 2012; Xiong et al., 2017; Zhou et al., 2014).

The second major source of non-destructive grass measurement error is HM prediction error. Several studies have highlighted the extent of RPM calibration error in predicting HM (Holshof et al., 2015; Klootwijk et al., 2019b; Sanderson et al., 2001), however error is unavoidable when performing any form of modelling. When implementing a grass measurement survey, it is necessary to quantify the level of error in order to justify the effort required to achieve a reasonably accurate result. In two preceding studies the authors have outlined and assessed RPM measurement and calibration error (Murphy et al., 2020a, 2020b). However, both of these errors are not static and will vary randomly within a certain probability distribution between measurements. Furthermore, increasing measurement rate and effort should theoretically result in a decrease in error in accordance with the law of numbers. The probability, or risk, of measurement error could be predicted over a number of repeated iterations by a method known as Monte Carlo simulation, which has been commonly applied to economic forecasting in agriculture (Grafton and Manning, 2017; Reidy, 1988; Shalloo et al., 2004).

There is scope for a DST that could combine total measurement survey error estimations with route optimisation procedures to enable the development of optimum grass measurement protocols. Baudracco et al., (2013) developed a DST incorporating a stochastic model to simulate pasture utilisation and economic performance based on animal genetic and pasture variable interactions. Romera et al., (2010) designed a DST to predict HM growth rates and reduce the requirement of physical data collection in New Zealand. Nakagami (2016) used Monte Carlo simulations to predict HM estimation error when evaluating a grass measurement method that minimised measurement effort.

This paper presents the Grass Measurement Optimisation Tool (GMOT) prototype, a DST designed to increase the accuracy and efficiency of grass measurement for farmers based on the findings from two previous studies (Murphy et al., 2020a, 2020b). The GMOT was designed to generate grass measurement protocols that optimise for both time and accuracy, dependent on the desired level of labour the farmer wishes to invest in a measurement survey. The following sections give an overview of the GMOT system, outline the methodology behind its development and analyse the potential benefits of the system.

2. Materials and methods

2.1. GMOT overview

The purpose of the GMOT was to create an interactive DST that would guide farmers on how to optimally measure their pastures. The tool was designed to indicate optimum target measurement locations and the shortest possible measurement route throughout pastures. The optimum route could then be followed using real-time GPS via an interactive map on the user's smart device. Measurement number, location and route were to be optimised for both accuracy and time. The GMOT prototype was developed to utilise basic pasture management and geo-spatial information to develop a spatially balanced and non-biased grass measurement protocol. Calibrations to predict HM that were built into the GMOT were capable of utilising pasture management information, such as fertilisation rates and the number of previously performed paddock grazing or cutting events, to increase HM prediction precision. The main considerations when designing the GMOT were to: 1) develop a grass measurement protocol to accurately predict the quantity and spatial variation of grazed grass in pastures in terms of HM, 2) optimise this protocol to minimize grass measurement time and labour requirements, 3) estimate overall measurement survey error, so that this can be accounted for when considering labour input and allocating HM to the herd and 4) evaluate the feasibility of the GMOT for on-farm use by means of a cost benefit analysis. The GMOT prototype can be accessed at the following link: https://messo.cit.ie/gmot

2.2. Data collection

The GMOT was developed based on data collected over three grazing seasons between March 2017 and October 2019 at the Teagasc Animal and Grassland Research Institute at Moorepark Fermoy Co. Cork, Ireland (50° 7́N, 18° 16́W). Data were collected on PRG cultivar controlled trial plots (5 m × 1.2 m) and grazed paddocks (1 ha), sown with treatments of PRG only and mixed swards of PRG and white clover (*Trifolium repens L.*; clover). Plots and paddocks were fertilised with nitrogen treatments ranging from 0 to 480 kg N ha^{-1} and were cut or grazed on average once every three to four weeks throughout the grass growing season (HM mean = 1,257 kg DM ha^{-1}, range = 35 – 4,082 kg DM ha^{-1}). On the controlled trail plots all of the available herbage was removed by cutting at regular intervals (28 days) to simulate grazing conditions, whereas on

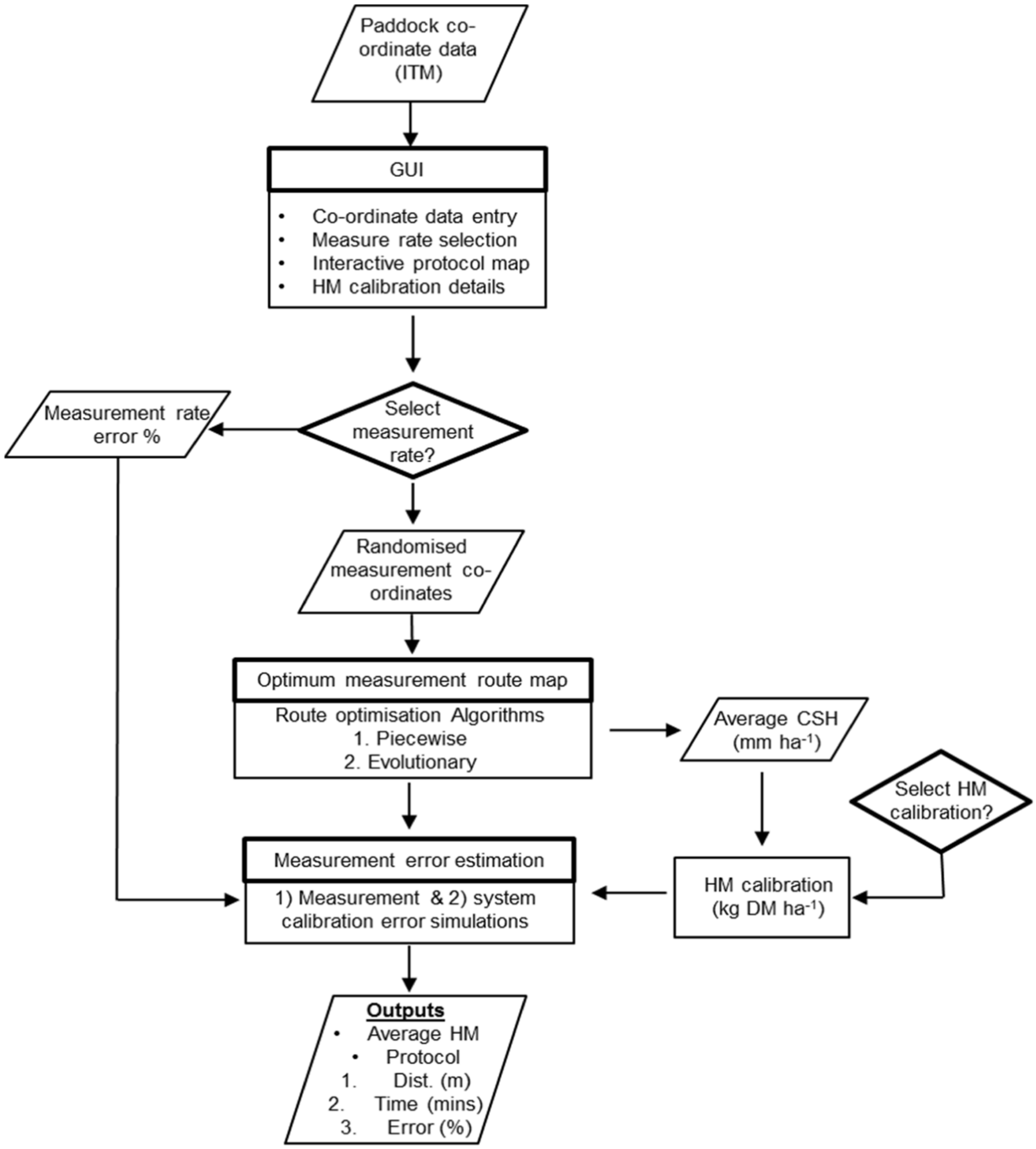

Fig. 1. Process flow diagram representing the main components of the GMOT system, Dist. = measurement route distance, GUI = graphical user interface, HM = herbage mass, ITM = Irish Transverse Mercator.

the paddocks herbage sub-samples were cut and taken prior to grazing (on average every three weeks), as outlined in (Murphy et al., 2020a). Trial plot data were used for HM calibration analysis purposes only (Section 2.5.2), whereas paddock data were used for calibration and spatial analysis. Grass CSH measurements were carried out and geo-referenced using an RPM developed by McSweeney et al., (2019). Herbage reference cuts were taken within the plots and paddocks using an Etesia mechanical mower (Etesia UK., Warwick, UK), with a targeted post cutting height of 40 mm. Paddock co-ordinates were recorded using a Trimble Catalyst GPS rover (*Trimble Inc., Sunnyvale, CA, USA*) operated in sub-meter mode (±30 cm), using the Irish Transverse Mercator (ITM) GPS compatible coordinate system (OSI, 2008).

2.3. GMOT user interface

The GMOT was developed using Visual Basics for Applications (Microsoft, 2010) to create a user friendly graphical user interface (GUI) designed in the form of an interactive paddock map based on the ITM co-ordinate system. A process flow diagram of the GMOT system can be viewed in Fig. 1.

2.3.1. GMOT inputs

2.3.1.1. Paddock co-ordinates and measurement rate. The main user inputs that were developed within the GMOT were the boundary co-ordinates (ITM) of the paddock selected for measurement along with user specified entry and exit points, which were designed in a manner that they could be copied or uploaded from an external GPS or GIS source. The GMOT was then programmed to generate an interactive map outlining the paddock boundaries in grey, along with alphabetically labelled corner points, as seen in the GUI outlined in Fig. 2. The longitudinal length of the paddock is then divided into a number of even strata, specified by the user, enabling RSS to be applied. Optional user inputs for the sampling protocol are outlined in the 'Measurement Protocol Details' section on the right hand side of the GUI in Fig. 2. The first option specifies the desired paddock measurement rate, which ranges between 1 and 32 ha^{-1}. Once the measurement rate is selected an equal number of random target measurement locations are allocated within the boundary limits of each strata. This was programmed using a uniform random number generator to select random co-ordinates, enabling RSS to performed, resulting in a spatially balanced and non-biased

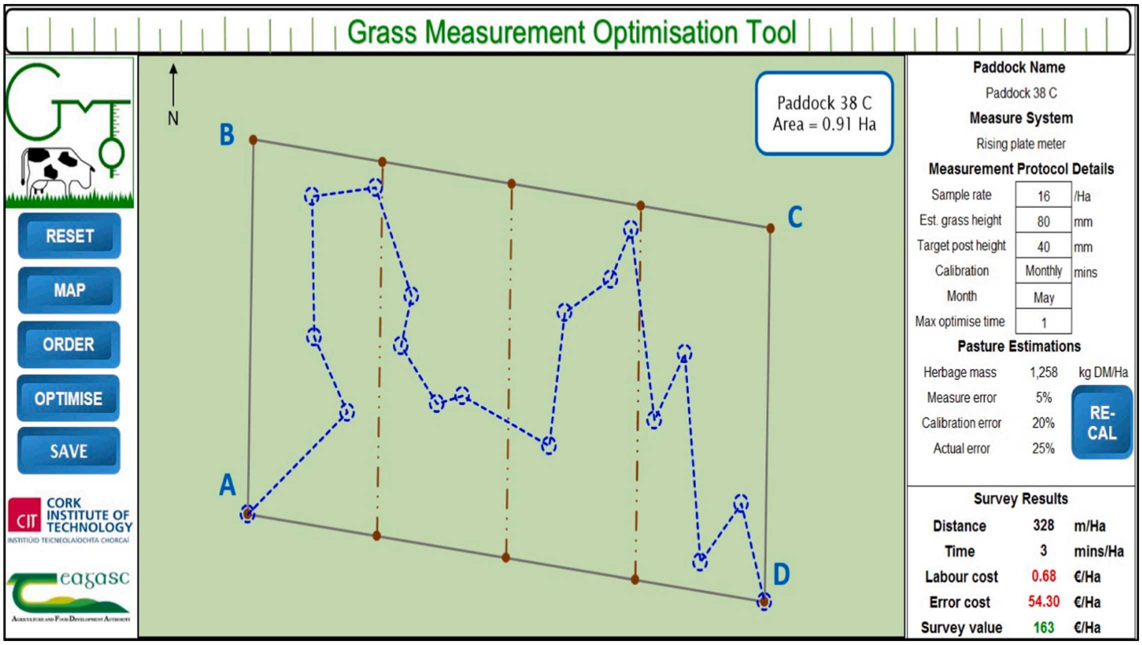

Fig. 2. GMOT graphical user interface, including interactive map of Moorepark paddock. An optimised measurement route is represented by the blue dashed line. Paddock strata are outlined by brown dashed lines and paddock boundaries are outlined in grey.

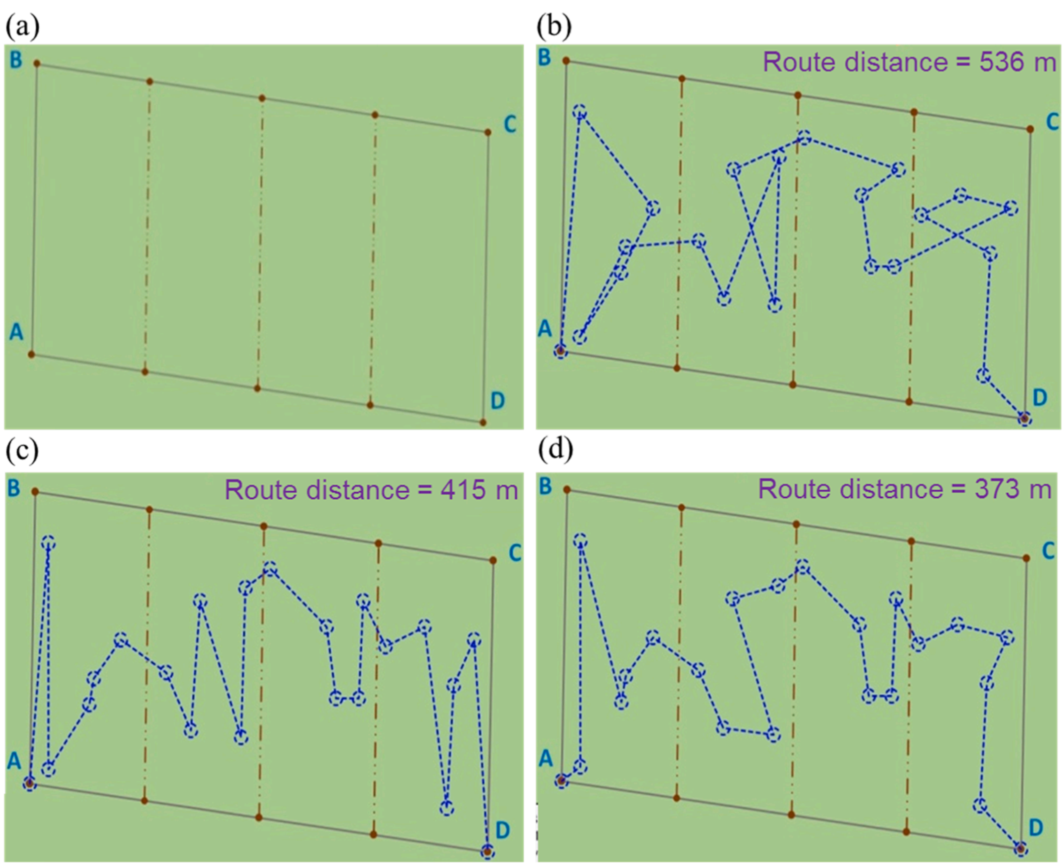

Fig. 3. GMOT interactive measurement route map outputs, including; (a) basic ITM coordinate map of Moorepark paddock (area = 1 ha), (b) random target measurement locations for 20 measurements ha^{-1} and random measurement route, (c) longitudinal ordered measurement route and (d) optimised measurement route.

estimate of average CSH as outlined in Murphy et al. (2020a). A randomised walking route was then created as a line series connecting the target measurement locations. The measurement route is represented by the broken blue line in Fig. 2.

2.3.1.2. Compressed sward height estimates. The second required GMOT user input detail is estimated average CSH, this value may be an approximate visual estimate inputted by the user prior to measuring to aid protocol design. The initial estimate can be updated for more accurate HM analysis with recorded values for each targeted measurement location once the survey is complete. The CSH inputs are used to estimate HM using calibrations developed by Murphy et al. (2020b), although these calibrations can be changed within the system settings to meet changes in seasonal, regional, or measurement system requirements. Predicted HM is displayed at the top of the 'Pasture Estimations' section of the GUI. The value of HM measured and the labour cost can also be specified by the user to allow for cost benefit analysis of each measurement survey.

2.3.2. GMOT outputs

The main output from the GMOT is the optimised measurement route map indicating the specified number of target measurement locations and optimum walking route, which is the shortest practical route that the farmer can travel when measuring a paddock. The first step in optimising the route involves ordering the measurement route, which arranges the target measurement location visitation order in terms of longitudinal co-ordinates. The second step requires optimising the measurement route by activating the route optimisation algorithm, which minimises route distance. GMOT map outputs of each of the optimisation steps can be viewed in Fig. 3 and the development of the algorithm behind the route optimisation process is discussed in further detail in Section 2.4. Additional GMOT outputs are outlined in the 'Survey Results' section in the bottom right hand corner of the GUI in Fig. 2 and include measurement route distance (m ha^{-1}), estimated walking time (mins ha^{-1}), and labour cost (€ ha^{-1}), along with the estimated cost benefit value of the measurement survey (€ ha^{-1}).

Walking time was calculated by factoring the route distance by the average human walking pace of 1.5 m s^{-1} (Minetti, 2000). Protocol cost was calculated by factoring time (hrs) by the user specified average dairy labour unit wage. The default value used was the Irish average dairy labour unit wage of €15 h^{-1} (Teagasc, 2018). The measurement protocol survey value indicated at the bottom of the 'Survey Results' section in Fig. 2 is the estimated total value of the survey in Euros per hectare (€ ha^{-1}), which was calculated by subtracting the estimated labour and error costs (€ ha^{-1}) from the value of the predicted HM. The value of predicted HM was calculated by placing a value of €0.173 on each kg of HM measured on the basis of the estimated net HM value presented in Hanrahan et al., (2018). Survey errors were initially estimated as a percentage of predicted HM, before being converted to kg DM ha^{-1} and factored by €0.173 kg^{-1} ha^{-1} to estimate survey error cost. Survey error estimates are discussed in further detail in Section 2.5. The default HM value can be adjusted within the GMOT to predict survey values in accordance with regional figures.

2.4. Measurement protocol route optimisation process

The GMOT was designed to minimise sampling time and labour input using an in-built optimum route finding algorithm. The algorithm calculated the shortest route that encompassed all randomly selected target measurement locations between user specified paddock entry and exit points. Total measurement route distance was determined as the sum of the combined distances between the paddock entry point, each target measurement location and the exit point. This was calculated using Eq. (1)

$$\Delta l = \sqrt{(\Delta x^2 + \Delta y^2)} \tag{1}$$

where Δl is the distance (m) between consecutive measurement locations, Δx is the ITM longitudinal difference between consecutive measurement locations and Δy the difference in latitude.

2.4.1. Piecewise algorithm

The first step of the route optimisation process is initiated by ordering the route using a piecewise algorithm (PA). The PA was programmed using an ordering function, which ordered the measurement route according to the longitudinal co-ordinates of each of the randomly selected target measurement locations. The PA algorithm significantly reduces the measurement route distance by removing any crossover points, as seen in Fig. 3(c).

2.4.2. Route optimisation algorithm

The second step of the route optimisation process is performed by a genetic algorithm (GA). The GA was designed on the basis of an open tour TSP that incorporates an evolutionary GA. The TSP involves selecting an optimum route that incorporates a number of target locations within a tour between a defined start and end point in the shortest possible path (Haupt and Haupt, 2004). The first step in applying this theory to optimise the GMOT measurement route involved determining the distances between the entire set of randomly selected target measurement locations. This was programmed in form of a distance matrix (Appendix A) that calculated the distance between all randomly selected co-ordinates for each sample rate using Eq. (1), as in similar studies (Jiang, 2010; Rasmussen, 2011).

The next stage programmed into the route optimisation algorithm involved coding a GA to find the optimum order in which to visit each randomly generated measurement location. The logic in employing a GA for this process was that manually calculating the distance of all possible route combinations that would encompass all measurement locations and subsequently selecting the shortest route was not feasible. The number of all possible route combinations with fixed start and end points for a selected measurement rate n is defined by Eq. (2) (Haupt and Haupt, 2004).

$$\frac{n!}{2} \tag{2}$$

where n is the selected measurement rate.

For example, with a recommended rate of 24 measures ha^{-1} there are 3.1×10^{23} possible route combinations.

The initial random route distance was calculated using the distance matrix. The route distance was then programmed to be ordered longitudinally once the PA was activated, as described in the previous section. The route distance, defined by the GA cost function in Eq. (3) below, was then set as the objective to be minimised by changing the route order.

$$c = \sum_{n=0}^{N} \sqrt{(x_n - x_{n+1})^2 + (y_n - y_{n+1})^2} \tag{3}$$

where (x_n, y_n) are the co-ordinates of the n^{th} measurement point visited, c is the measurement protocol cost in terms of walking distance (m), and N is the selected measurement rate.

The main component of the GA is the Excel evolutionary solver, which was coded via VBA and used to search a vast number of possible route combinations to determine an optimum solution. The GA was programmed to continue searching the solution space for the shortest route until specified stopping criteria were adhered to. The GA was designed to find the best practical solution within the limits of the stopping criteria, which may not always be the global optimal solution. Two significant GA parameters are population size and mutation rate. Population size refers to the number of random possible trial route solutions that the GA will initially select to begin the optimisation process. The mutation rate refers to the randomness introduced when mating the most optimum solutions (Abdoun et al., 2012; Keller et al., 2016). The main GA stopping criteria were convergence, max run time, max iteration number, precision, max sub-problems and max time. Convergence refers to the set limit at which the GA will stop when 99% or more of the selected population have relative fitness values below this level. Max time refers to the time limit that the GA will run for, the iteration

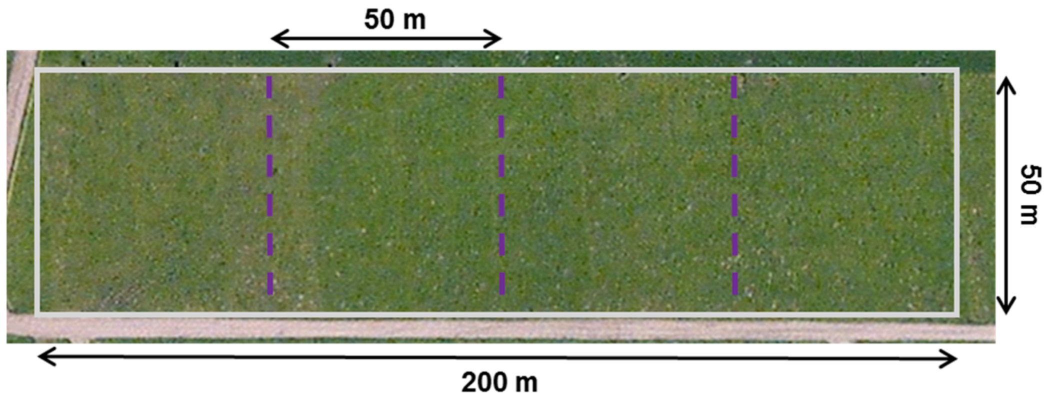

Fig. 4. Moorepark 1 ha trial paddock used for route optimisation analysis. The paddock boundary is outlined in grey and GMOT strata divisions are outlined by purple dashed lines.

number is the max number of possible route combinations the GA will assess, the precision is the accuracy to which the objective needs to be satisfied, max sub-problems is the max number of more optimum solutions the GA will explore and max time is the time limit at which the GA will stop if it does not find a better solution than the previous (Fylstra et al., 1998; Microsoft, 2020). The selected GA parameters outlined in Appendix A, were similar to those outlined by Jiang (2010) and Rexhepi et al., (2013) who also utilised the VBA solver to optimise similar TSPs. The main components of the GA are summarised by the pseudocode presented in Appendix A.

The GMOT optimisation process may take several hours (0–9 hrs) to complete on conventional computers depending on the number of measurements selected, due to the computational complexity of the TSP as previously discussed. An option to place a time constraint on optimisation was programmed into the GMOT and the user can change the max simulation run time limit, however, this may result in less optimum route solutions. The GMOT was designed to be used in the field on handheld devices via a virtual private network link to a computer with greater processing power, with the aim of completing the optimisation process within a practical time period. Finally, it is recommended that a protocol be re-generated for each new survey to ensure that the selected measurement locations remain random and non-biased.

2.4.3. GMOT route optimisation simulation analysis

The benefits of the route optimisation process, in terms of reducing route distance, were evaluated by performing route optimisations on RSS target measurement locations on a 1 ha paddock in Moorepark (Fig. 4) for a range of measurement rates (N = 1, 2, 4, 8, 16, 24, 32). The paddock was divided into four even strata based on its ITM co-ordinates and the optimisation process was simulated for 30 random target measurement location generations for each measurement rate. Randomised route distance values were recorded for each simulation along with the PA and GA optimised routes. All route values were averaged across all simulations to determine the overall distance reduction value for each stage of the GMOT route optimisation process.

2.5. Measurement survey error estimates

Protocol error estimations made by the GMOT are indicated in the 'Pasture Estimations' section on the right hand side of the GUI in Fig. 2. As measurement and calibration errors may vary considerably between measurements, estimated values were generated stochastically based on Monte Carlo simulation analysis.

2.5.1. Measurement error

Sampling of grazed paddocks was conducted on 13 dates over a grass growing season in Moorepark. Stratified blanket CSH sampling (n = 320 ha^{-1}) was conducted within paddocks on each measurement date to determine measurement error probability distributions, as outlined in Murphy et al. (2020a). Average measurement rate error was expressed as a percentage of 'true' mean CSH, taken as the average of all 320 CSH measurements performed on each date. Randomised error simulations were performed by randomly selecting a number of CSH measurements taken on each date to estimate mean CSH; this mean was then compared to the 'true' mean of all 320 measurements to determine prediction error. Random measurement selections were taken in even numbers from each strata within the paddocks to coincide with each measurement rate. This was repeated for 100 iterations for each measurement date creating a Gaussian frequency distribution with 1300 averaged error values for each measurement rate across the growing season. Error distributions for each measurement rate can be viewed in Appendix B. Simulated measurement error datasets underwent Shapiro-Wilk tests for normality and if $P < 0.05$ then values $> 3\sigma$ were considered outliers and removed (< 2%). Normality tests were repeated once outliers were removed and if conditions of normality were not met, data transformations were performed. The mean and standard deviation of each measurement rate error distribution was then used to program stochastically simulated error values to be applied to each measurement generated by the GMOT, to predict measurement error for each survey.

2.5.2. Herbage mass calibration error

Error for predicted HM was simulated in a similar manner to that of measurement error. Probability distributions of calibration error were determined using CSH and HM data collected over three growing seasons, along with residual HM prediction errors from calibrations developed as part of a previous study (Murphy et al., 2020b). Error values were calculated in terms of kg DM ha^{-1} by comparing predicted HM, from CSH measurements using annual HM and monthly HM calibrations, with reference HM values from herbage cuts.

Error was expressed in terms of relative prediction error (RPE), which is the root mean squared error (RMSE) expressed as a percentage of the actual mean HM value recorded from herbage reference cuts. RMSE was calculated using the following Eq. (4).

$$RMSE = \sqrt{\frac{\sum_{i=1}^{N}\left(HM_i - \widehat{HM}_i\right)^2}{N}} \tag{4}$$

where N, is the number of data points and HM_i and $\widehat{HM}_i$ are the observed and predicted values of HM for the i^{th} data point.

Predicted HM error values were then used to develop the Gaussian distributions shown in Appendix B, which were assessed and treated for normality as in Section 2.5.1. As for measurement error, calibration error distributions were used to program stochastically simulated error values to be applied to average predicted HM from each GMOT measurement survey to account for calibration error.

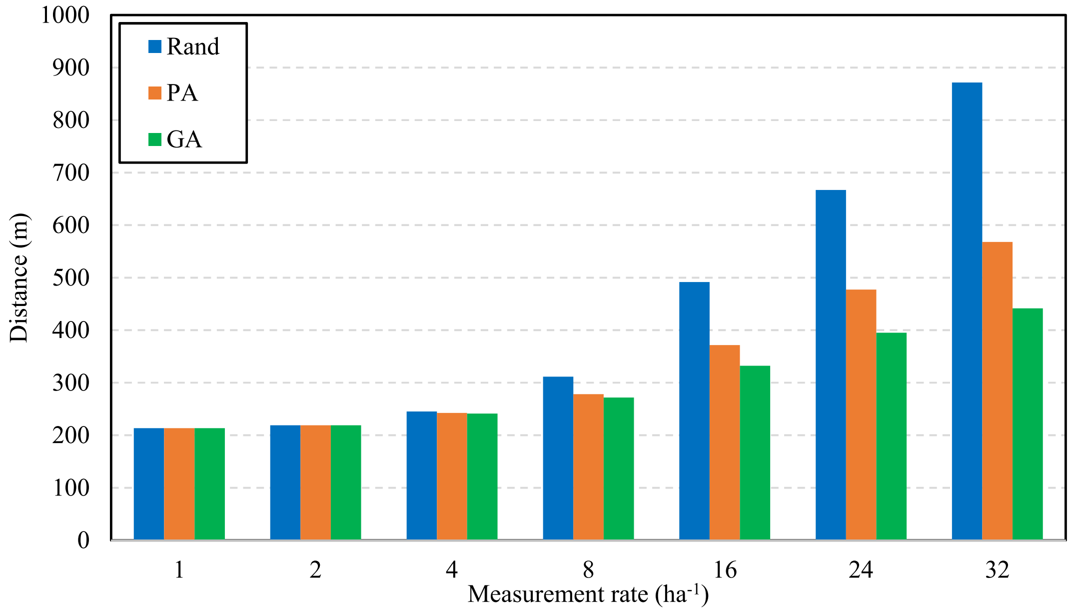

Fig. 5. Averages of 30 simulated measurement route distances of each random stratified measurement rate for randomised (Rand), piecewise algorithm (PA) and genetic algorithm (GA) routes.

2.5.3. Herbage mass calibration model analysis

Calibration error is dependent upon the selected HM calibration for a survey, which has been reported as a large source of error for RPMs (Klootwijk et al., 2019b; Sanderson et al., 2001). Monte Carlo analysis was repeated for a number of different calibrations to investigate the effect of calibration error on overall actual survey error. The analysed HM calibrations included annual (28% RPE) and monthly (25% RPE) models from Murphy et al. (2020b) and a basic model with a 35% RPE. More accurate hypothetical models were further included within the Monte Carlo analysis to simulate the potential effects of using the GMOT with future grass measurement systems, which may have greater HM prediction accuracy. These included sufficient (10% RPE) and ideal (0% RPE) HM prediction models. The sufficient model with a target RPE of 10% was selected to investigate the recommendations made by Sanderson et al., (2001), who suggested that HM prediction error must be within 10% to be sufficiently accurate for feed budgeting. The ideal model represents a hypothetical future grass measurement technology capable of predicting HM without error.

2.5.4. Estimated actual survey error

The GMOT was designed to estimate overall actual grass measurement survey error by combining stochastic measurement and calibration error simulations based on the analysis outlined in the previous sections. Actual grass measurement survey error was estimated by combing predicted measurement and calibration error values. The combined potential effect of both error sources was predicted using Monte Carlo simulation. This involved simulating 1000 grass measurement surveys for each measurement rate and HM calibration, each with Gaussian simulated measurement and HM calibration errors, to estimate combined actual survey error values. A greater number of simulations than that of the route optimisation analysis (Section 2.4.3) was possible because the computational expense required was not as large. Percentage errors were calculated in terms of RPE of a mean CSH of 80 mm and HM value of 1,257 kg DM ha^{-1}, which were the average values recorded for these parameters on the plots and paddocks over the three year period of this study. Estimated average actual survey error across all simulations was then used to predict average estimated survey errors for individual measurement rates and HM calibrations.

Simulated surveys assumed a recording of CSH of 80 mm for each measurement. Stochastically simulated error percentages were then applied to individual measurements dependent on the selected measurement rate error distribution. Individual measurement values with simulated error were then used to estimate mean CSH, which was compared to the 'true' mean CSH (80 mm) to determine measurement RPE. Estimated mean CSH was then factored into each of the HM calibrations mentioned in Section 2.5.3 to predict HM. Stochastically simulated calibration error was then applied to the predicted HM value as in Section 2.5.2 resulting in a predicted HM survey value combining simulated calibration and measurement error. This enabled the prediction of measurement, calibration and combined actual survey error for each of the 1000 simulations for each measurement rate and HM calibration. Combining these findings with the route optimisation simulation results enabled a simulated cost benefit analysis of the GMOT system to be performed.

2.6. GMOT cost benefit analysis

An evaluation of the GMOT system was carried out by applying the results of both error and route optimisation simulation analyses to design hypothetical grass measurement protocols for a typical Irish grass based dairy enterprise. The hypothetical farm scenario was based on average national figures taken from Teagasc's National Farm Survey (Teagasc, 2018) and recent published figures from PBI (Maher et al., 2019; O' Leary and O' Donovan, 2019). Grass measurement practices on the farm were assumed to be in accordance with current best practice guidelines. The farm was envisaged to utilise on average 13 tonnes ha^{-1} and perform 30 grass walks per annum, in accordance with data from the best performing commercial farms on PBI. The farm area was assumed to be 38.3 ha, which is the average Irish milking platform size. The net profit value placed on each tonne of HM measured, and therefore assumed to be utilised, was taken as €173 tonne ha^{-1} yr^{-1} (Hanrahan et al., 2018). The cost of each survey was determined by factoring measurement route distance (m ha^{-1}) by survey time (hrs) and labour cost (€ ha^{-1}), as mentioned in Section 2.3.2. Reductions in survey error were assumed to result in proportional increases in grass utilisation. The monthly HM calibration mentioned in Section 2.5.3 was used to predict HM, as this had the lowest RPE of all RPM calibrations currently available for Irish grassland. A grass measurement cost benefit analysis was performed for the farm, assuming GMOT designed measurement protocols were adhered to for each grass walk, to evaluate the potential

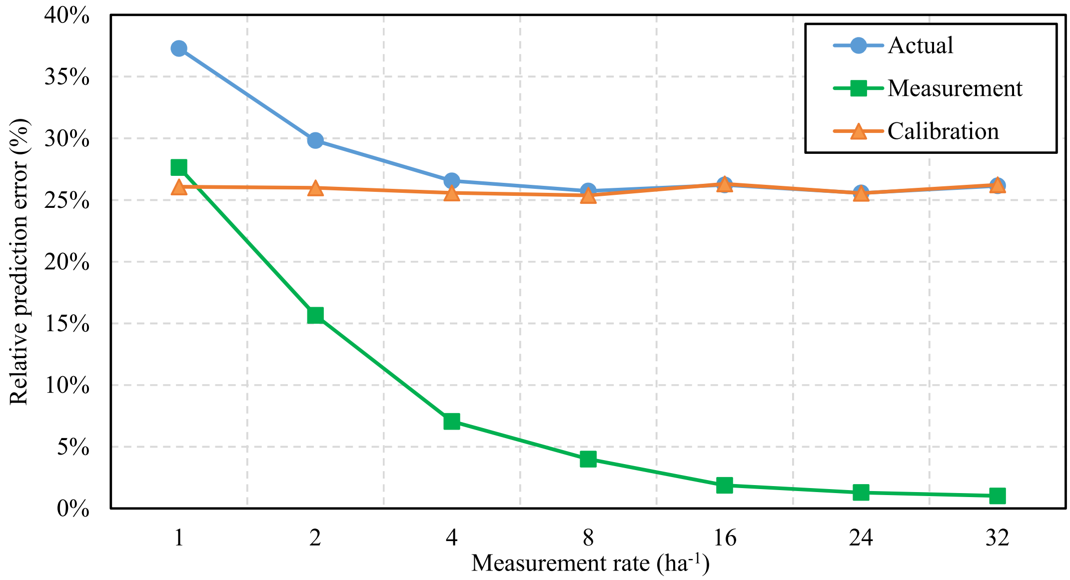

Fig. 6. Average values of Monte Carlo simulations (n = 1000) for measurement survey: actual, measurement, and calibration errors for each measurement rate.

financial benefits of the system in terms of increasing grass utilisation and reducing measurement labour on an annual basis.

3. Results and discussion

The following results and discussion are sub-dived into three main sections: 1) route optimisation analysis; where the results of the GMOT route optimisation algorithm simulations are outlined, 2) error analysis: the results from the GMOT error analysis simulations are described along with HM calibration model error analysis, and 3) GMOT system evaluation; an evaluation of the GMOT system is outlined for a typical Irish pasture based dairy farm.

3.1. Route optimisation analysis

The average distance of 30 simulated RSS routes for each measurement rate on the Moorepark trial paddock are outlined in Fig. 5. Route distances are presented in terms of the initial randomised route, the PA ordered route and the GA optimised route. At measurement rates of 1 ha^{-1} and 2 ha^{-1} there was no difference between any of the route distances as there is only one route option between the paddock entry point, randomised within strata target measurement locations, and exit point. The first considerable reduction in route distance was achieved at a measurement rate of 8 ha^{-1} with an initial PA reduction of 33 m (11%) and a total reduction of 40 m (13%) when the GA was implemented. As the number of possible route options increased, the benefit of both the PA and GA in terms of distance reduction increased proportionally in accordance with Eq. (2). Maximum reductions in measurement distance occurred at the rate of 32 ha^{-1} for both the PA (303 m, 34.9%) and the GA (430 m, 49.4%). At the optimum measurement rate of 24 ha^{-1} recommended in Murphy et al. (2020a), the PA reduced measurement route distance by 190 m (28.5%) and employing the GA resulted in a total reduction of 272 m (40.7%). The average CPU processing time required to run the GA optimisation process on a computer with an Intel Xeon(R) 2.3 GHz processor and 128 GB RAM ranged from 2.81 hrs at 8 measures ha^{-1} to 5.01 hrs at 32 measures ha^{-1}. For practical use of the GMOT in the field, remote access to a high speed cloud computation facility would be necessary to run the optimisation process within a practical time period of several minutes.

The piecewise algorithm was efficient at reducing distance within one second of CPU time for all sampling rates above 2 ha^{-1}. Preliminary tests in the development stage of the GA indicated that the optimisation process worked more efficiently when the route was initially ordered using the PA, as the objective function and initial population were much closer to the optimum. Sathyan et al., (2015) and Xiong et al., (2017) used similar route ordering techniques in attempting to solve TSPs for unmanned vehicle route optimisation.

The GA, was effective at reducing the measurement distance for all measurement rates greater than 2 ha^{-1}, which is in agreement with a number of other studies (Jiang, 2010; Patterson and Harmel, 2003; Rasmussen, 2011) and all GA simulations converged to within the specified parameter limits outlined in Section 2.4.2.

3.2. Error analysis

3.2.1. Error frequency distributions

Gaussian error distributions for all measurement rates between 1 ha^{-1} and 8 ha^{-1} were found to be negatively skewed ($P < 0.05$) (Appendix B) indicating that measurement error was biased towards overestimating mean CSH. To meet conditions of normality, a constant was added to each dataset and a square root transformation performed. Likewise, the frequency distribution for HM error was also negatively skewed ($P < 0.001$) (Appendix 2) and adding a constant with a log transformation enabled conditions of normality to be met. Negative HM error skews may have also resulted from the overestimation of mean CSH values, which were used to predict HM. Barthram et al., (2005), found that sward height measurements within grazed pastures were typically positively skewed as a result of disproportionately high patches of grass caused by grazing effects and recommended a log normal distribution to best fit this data. The negative HM skews found in this study may be linked to overestimation of mean CSH caused by the accidental measurement of patches of less palatable tall grass within the sward that surrounded dung pats or had gone to seed head, which were rejected by grazing animals. Likewise, overestimations could have been caused by depressions in the soil surface, resulting from animal poaching by grazing in wet weather. These phenomena may explain some of the large overestimations in CSH and HM, which caused the negative skews within the error frequency distributions developed as part of this study.

3.2.2. Error simulation results

Average error analysis results of Monte Carlo simulations for simulated measurement surveys for each measurement rate are presented in Fig. 6. Measurement survey RPE is presented in three forms: 1) measurement error; estimated from the selected number of measurements

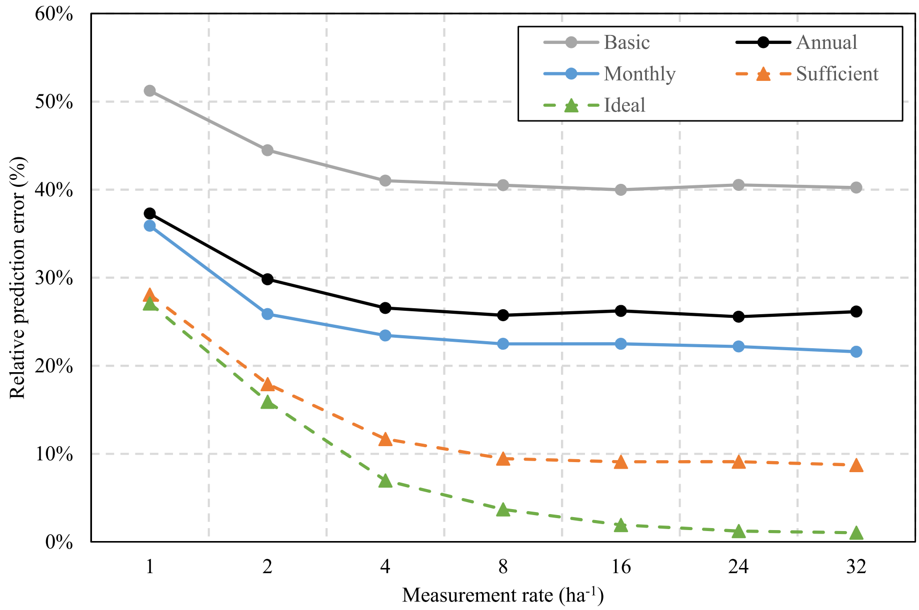

Fig. 7. Monte Carlo simulated grass measurement actual survey error (n = 1000) for basic (35% RPE), annual (28% RPE), and monthly (25% RPE) rising plate meter calibrations, along with hypothetical herbage mass prediction models for sufficient (10% RPE) and ideal (0% RPE) future grass measurement systems.

ha^{-1}, 2) calibration error; based on the RPE of the selected HM prediction model and 3) actual error; which is the combination of both measurement and calibration errors.

Mean calibration error (25.9%) was more than three times mean measurement error (8.4%) and was relatively constant across measurement rates. Measurement error decreased exponentially as measurement rate increased, as reported in previous studies (Hutchinson et al., 2016; Murphy et al., 2018, 2020a). From Fig. 6 it can be observed that the largest reduction in measurement error (11.9%) occurred as the measurement rate increased from 1 – 2 measurement ha^{-1}. There were more gradual reductions in error between 2 - 4 measurements ha^{-1} (8.6%), 4 – 8 measurements ha^{-1} (3.1%), and 8 – 16 measurements ha^{-1} (2.1%). The relative reduction in measurement error was substantially lower as the measurement rate increased from 16 - 24 measurements ha^{-1} (0.6%) and 24 – 32 measurements ha^{-1} (0.3%). Mean actual measurement error for the RPM across all measurement rates was 28.1%, which is similar to findings made by the authors in a previous study (Murphy et al., 2020b) along with further findings made by Klootwijk et al., (2019b) and Sanderson et al., (2001). Nakagami (2016) using Monte Carlo simulations, estimated that HM prediction errors could be maintained within 20% of the mean using two RPM measurements per paddock on Japanese grasslands, however, discovered that error increased considerably when this method was validated in a field study.

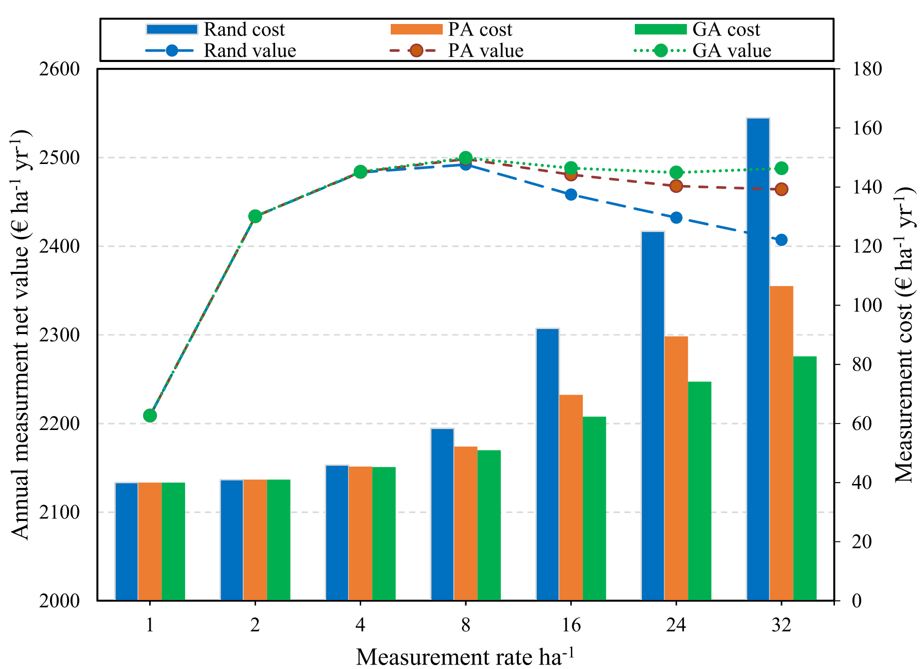

Fig. 8. Cost benefit analysis of random (Rand), piecewise algorithm (PA), and genetic algorithm (GA) generated measurement routes for different measurement rates designed by the GMOT. Analysis was based on an average sized dairy farm (38.3 ha) following current best practice grass measurement guidelines and utilising 13 tonnes DM ha^{-1} yr^{-1}.

Similar to measurement error, the largest decrease in actual error was observed as measurement rate increased from 1 - 2 measurements ha^{-1} (7.46%), with more gradual decreases occurring at 4 (3.3%) and 8 (0.8%) measurements ha^{-1}. Actual error became relatively constant at just over 25% at rates between8 – 32 measurements ha^{-1}. The minute decreases in actual error as the measurement rate increased from 8 – 32 measurements ha^{-1} were most likely a result of the relatively high calibration error (25.9%) overshadowing the minimal reduction (3%) in measurement error observed between these rates. Therefore, there is minimal benefit in increasing RPM measurement rates above 8 ha^{-1}. This measurement rate is lower than the sampling rate of 24 measurements ha^{-1} recommended by the authors in a previous study, which focused solely on measurement error (Murphy et al., 2020a).

3.2.3. Herbage mass calibration model error analysis

The findings of this study confirm that HM calibration accuracy is the largest source of error with regard to the RPM. Several studies have shown that the selection of a suitable RPM HM calibration model impacts on overall HM measurement error and ultimately grass budgeting costs (Holshof et al., 2015; Rayburn et al., 2017; Sanderson et al., 2001). Furthermore, there is scope for improving the overall accuracy of the RPM by developing more accurate sward and seasonal specific calibrations using novel modelling techniques (Klootwijk et al., 2019b; Murphy et al., 2020b). In this study the authors wanted to investigate the relationship between HM calibration accuracy, measurement rate and actual survey error, to establish if reducing model error could greater utilise the route optimisation potential of the GMOT. Fig. 7 presents an analysis of the effect of HM calibration error on actual survey error. This analysis shows that even for a hypothetical sufficiently accurate HM prediction model with 10% RPE, there is only a small decrease in actual error (0.4%) when the measurement rate is increased from 8 - 16 measurements ha^{-1}, with negligible decreases in error as the measurement rate is further increased beyond 16 measurements ha^{-1}. For the hypothetical ideal HM prediction model, potential reduction of actual error increased (1.8%) between 8 - 16 measurements ha^{-1} and there was a further small reduction in error (0.7%) between 16 - 24 measurements ha^{-1}. Beyond 24 measurements ha^{-1}, error reductions for the ideal HM prediction model were negligible. This is due to the natural heterogeneity of the sward within a paddock. Even if an ideal grass measurement system was employed, blanket sampling would be required in order to completely eliminate prediction error. These findings are in agreement with an earlier study by the authors (Murphy et al., 2020a). Moreover, these results indicate that a considerable increase in HM calibration accuracy is required to greater utilise the route optimisation potential of the GMOT and higher GMOT measurement rates may become more feasible with the onset of future grass measurement systems with lower RPE values. These results further indicate that there is little benefit, in terms of error reduction, in measuring at a rates > 8 ha^{-1} unless a measurement system with much greater HM prediction accuracy is developed in the future.

3.3. GMOT system evaluation

Cost benefit analysis predictions for a typical Irish dairy farm following best practice grass measurement guidelines and using the GMOT to design each grass walk are presented in Fig. 8. Fig. 8 details annual measurement costs based on different GMOT designed protocols, which vary in terms of measurement rate ha^{-1} and RSS route. Further illustrated is the net value (€ ha^{-1} yr^{-1}) of each measurement rate, which is the potential value of HM utilised minus survey error and labour cost. The same calculation process is used to generate the survey value output in the GMOT. Ballari et al., (2012) used a similar approach to optimise sampling locations for wireless sensor networks by estimating and minimising the cost of producing inaccurate predictions, with the ultimate aim of increasing the value of measured spatial information. Fig. 8 outlines how measurement cost is proportional to HM utilisation. As measurement rate increases and error decreases, in accordance with Fig. 6, measurement cost rises as the survey route becomes longer. Protocols designed at the rate of 1 measurement ha^{-1} were assumed to be the base reference of survey value, where the farmer is currently utilising 13 tonnes of DM ha^{-1} throughout the year by using simple grass measurement techniques with no rigid protocol. Measurement value peaked at €2500 ha^{-1} yr^{-1} for the GMOT GA designed protocol at a measurement rate of 8 ha^{-1}, with a corresponding measurement cost of €73 ha^{-1} yr^{-1}. The largest increases in measurement value (€290 ha^{-1} yr^{-1}) were achieved by increasing the measurement rate from 1 – 8 ha^{-1}. As the measurement rates increased from 8 – 32 ha^{-1}, increases in measurement costs coupled with lower decreases in survey error resulted in reduced net measurement values for all protocols. The cost reduction benefit of both the PA and GA designed routes were negligible at measurement rates 1 – 4 ha^{-1} and became more evident as the measurement rate increased above 8 ha^{-1}. At 8 measurements ha^{-1} the PA and GA reduced measurement costs by €6 ha^{-1} and €7 ha^{-1} per annum, respectively. Maximum measurement cost reduction for all GMOT GA designed routes was achieved at the rate of 32 measurements ha^{-1} with reductions of €81 ha^{-1} yr^{-1} (50%) in comparison with the random route and €24 ha^{-1} yr^{-1} (22%) for the PA route. The GMOT GA designed route at a measurement rate of 8 ha^{-1} increased net measurement value by €11,131 per annum across the average size dairy farm (38.3 ha) by reducing survey error and cost. Survey error reductions resulted in an increase in grass utilisation of 1.7 tonnes DM ha^{-1} yr^{-1}, whereas measurement cost was curtailed by €7 ha^{-1} yr^{-1}.

GA designed routes reduced measurement cost by 13% at the optimum measurement rate of 8 ha^{-1} and cost reduction became greater as measurement rates increased, which further highlights the greater potential benefits of GA designed routes if HM calibration accuracy is increased. The net decrease in measurement value above the rate of 8 measurements ha^{-1} was a result of negligible decreases in survey error due to the overshadowing effect of the relatively high calibration error, as previously discussed in Section 3.2.2. Although if calibration error was substantially reduced it may become feasible to increase the optimal measurement rate, thus increasing the value of GA designed routes. The RSS strategy and geo-statistical approaches upon which the GMOT is designed are dynamic and will be applicable to many future grass measurement technologies with potentially lower HM prediction errors.

3.4. GMOT benefits

The benefits of the outputs from the GMOT include removing operator subjectivity along with increasing the precision and efficiency of both grassland measurement and management. By using the GMOT farm managers could estimate the accuracy of their measurements, enabling margins of error to be accounted for when allocating areas of herbage to the herd. Furthermore, farmers could accurately predict the time inputs required and allocate sufficient time in their weekly schedule to achieve the desired level of accuracy from their farm walk. Conversely, GMOT designed measurement routes would require the use of a smart device and may take more time to follow in comparison to simple pasture measurement methods, such as measuring by transects. The farmer would also need an internet connection for remote access to a cloud based server to run the route optimisation process. Moreover, the objectivity of measurement location selection may be limited by the precision of the GPS system used in tandem with the GMOT. However, the survey value calculated by the GMOT highlights the financial incentive of regular and precise grass measurement and may entice farmers to conduct more grass walks throughout the year. Additionally, the GMOT outputs enable grassland measurement surveys to be outsourced at a price based on predicted time, effort and accuracy. Moreover, using the GMOT when outsourcing measurements would ensure that a predetermined protocol that maintains measurement standards is adhered to. The GMOT was designed primarily for Irish PRG dominant grazing production systems, however, the sampling principles upon which it was designed are applicable to any pasture based system and could further be applied to 'zero grazing' systems, which are more common within the EU. Moreover, further reductions in optimum measurement rate and time could be possible on 'zero grazing' systems as a result of greater sward homogeneity, due to absence of grazing effects. Furthermore, region and species specific HM calibrations can be uploaded to the GMOT to enable the analysis of different sward types.

The RSS strategy employed by the GMOT enables sward heterogeneity to be accurately predicted by geostatistics. RSS enables geostatistical procedures, such as Kriging interpolation, to be employed to generate yield maps using the geo-tagged measurement data outputs produced by the GMOT (Webster and Lark, 2012). This will enable further research into seasonal variation in sward heterogeneity and its effects on grass measurement precision. Furthermore, the geostatistical principles on which the GMOT is based are directly applicable to herbage sampling for quality analysis and soil sampling. The GMOT has multiple potential benefits with regard to facilitating the application of precision agricultural technologies to grassland farms, in areas such as targeted fertilisation and management, as outlined by Shalloo et al., (2018).

The findings of this study indicate that HM calibration is the largest source of RPM error once a robust measurement protocol is adhered to. The inbuilt GMOT HM calibrations can be modified according to region and season to reduce calibration error. These calibrations can be further updated in accordance with future research. Although the GMOT was designed in conjunction with the RPM, the RSS and geostatistical principles upon which it is designed can be modified to work with a range of grass measurement systems. There is scope to utilise the design principles of the GMOT to enable the automation of grass measurement in the future, by either aerial or terrestrial unmanned vehicles, such as the pasture robot proposed by Manderson and Hunt (2013). This potential is outlined in a similar study by Xiong et al., (2017) who developed a terrestrial drone for targeted weed eradication, which followed TSP designed optimised routes.

Results from this study indicate how measurement rate and effort can be reduced compared to rates recommended by previous studies (Hutchinson et al., 2016; Klootwijk et al., 2019a; Murphy et al., 2020a) once GMOT designed routes are followed, thus highlighting the tool's potential to reduce grass measurement labour inputs. Although CPU time was too large for practical real-time optimisation in the field using the GA coded in VBA; this software makes the GMOT prototype available to a wide range of users at minimal cost. The authors hope the availability of this software will promote the potential benefits of the GMOT and lead to its development for use in industry. The authors envisage that this prototype will lead to a DST application that will promote more accurate, efficient, and frequent grassland measurement.

4. Conclusion

To conclude, the main findings from this study on developing a grass measurement optimisation tool to increase pasture management precision and efficiency were;

- A GMOT prototype was developed to promote more accurate and efficient grass measurement
- The GMOT utilised random stratified sampling, GPS coordinates, a genetic algorithm and sward specific herbage mass prediction calibrations to optimise measurement accuracy and time
- GMOT outputs include optimised measurement route maps along with estimated measurement survey financial value, cost, error and time
- Monte Carlo analysis of GMOT outputs found that the main source of error for the rising plate meter was calibration error, which was more than three times larger than measurement error
- Cost benefit analysis of GMOT outputs showed a diminishing rate of returns in net measurement value when performing more than 8 measurements ha^{-1}
- GMOT outputs enable optimal grass measurement of pasture by performing 8 measurements ha^{-1} in a random stratified manner using the rising plate meter
- The geostatistical design principles of the GMOT are dynamic and can be applied to a range of pasture measurement technologies.

CRediT authorship contribution statement

D.J. Murphy: Methodology, Software, Conceptualization, Formal analysis, Data curation, Writing - original draft. **B. Brien:** Validation, Resources, Writing - review & editing, Supervision, Project administration, Funding acquisition. **M.D. Murphy:** Resources, Writing - review & editing, Supervision, Project administration, Funding acquisition.

Declaration of Competing Interest

The authors declare that they have no known competing financial interests or personal relationships that could have appeared to influence the work reported in this paper.

Acknowledgements

This research was part of the ICT – AGRI GrassQ project (Project ID: 35779) and was supported by the Irish Department of Agriculture, Food and the Marine and the European Commission's ERA-NET, ICT – AGRI scheme as part of the Horizon 2020 programme.

Appendix A

(See: Table A1) and (See: Table A2)

Algorithm 1. (*Measurement route optimisation*)

```
input: Paddock co-ordinates, paddock entry point and exit point
output: measurement co-ordinates (C), measurement route (r),route distance (D), sample route map
  select: strata number (N)
    calculate: strata boundaries S_N = (Sx_i,y_i, Sx_j,y_j, … Sx_N,y_N)
  select: measurement rate number (n)
  randselect: C =(x_i,y_i, x_j,y_j, … x_n,y_n)
      for min(Sx_ij,y_ij) ≤ x_ij,y_ij ≥ max(Sx_ij,y_ij) \\within strata bounds
  define: r = {1,2,3,…n) for all \\assign numerical order value to each measurement point
    calculate: D \\ distance matrix between all measurement points
      sort: r 0 → x \\ sort co-ordinates by latitude (piecewise algorithm)
        for: r minimize D \\by changing measurement point route order
          do until: r = convergence criteria
            stop: once convergence criteria satisfied
  print: route map
  end
```

Table A1
Distance matrix for a rate of 24 measurements ha^{-1} used to calculate distances (m) between randomly selected targeted measurement co-ordinates (ITM). Target measurement locations are numbered in order of longitudinal values from left to right in the North direction.

Target measurement locations	Entry	1	2	3	4	5	6	7	8	9	10	11	12	13	14	15	16	17	18	19	20	21	22	23	24	Exit
Entry	0.0	20.1	42.7	22.1	54.9	38.4	34.3	66.8	81.1	58.3	69.2	67.3	80.2	113.1	136.5	112.1	110.1	122.9	145.1	161.5	183.1	152.1	185.3	158.1	168.1	202.4
1	20.1	0.0	30.1	6.4	39.1	18.4	14.8	47.5	64.3	42.2	57.1	48.3	68.1	101.0	123.1	95.7	96.0	106.7	132.6	148.0	170.7	140.3	171.1	145.7	155.5	190.8
2	42.7	30.1	0.0	35.5	14.1	25.0	21.9	34.2	40.0	17.7	27.2	33.1	38.2	71.3	94.1	70.0	67.5	80.7	103.1	119.1	141.2	110.5	142.7	116.2	126.1	161.0
3	22.1	6.4	35.5	0.0	43.1	19.3	17.1	48.8	67.5	46.0	62.1	50.0	73.0	105.7	127.3	98.9	100.1	109.9	137.2	152.2	175.1	145.0	175.0	150.2	160.0	195.5
4	54.9	39.1	14.1	43.1	0.0	26.9	26.5	22.1	26.4	3.6	21.4	20.4	31.3	63.1	84.2	57.3	57.0	68.2	94.2	109.1	132.1	102.2	132.1	107.2	117.0	152.6
5	38.4	18.4	25.0	19.3	26.9	0.0	5.1	29.5	49.0	29.1	47.9	30.7	58.2	89.8	110.2	80.2	82.9	91.3	120.6	134.8	158.3	128.8	157.1	133.6	143.2	179.1
6	34.3	14.8	21.9	17.1	26.5	5.1	0.0	32.8	50.4	29.2	46.6	33.5	57.2	89.5	110.5	81.7	83.3	92.8	120.7	135.4	158.5	128.7	158.0	133.7	143.4	179.1
7	66.8	47.5	34.2	48.8	22.1	29.5	32.8	0.0	24.6	20.0	38.1	2.8	44.4	70.2	86.6	53.3	60.0	64.2	98.2	110.4	134.8	107.0	131.2	110.7	119.9	156.2
8	81.1	64.3	40.0	67.5	26.4	49.0	50.4	24.6	0.0	22.8	25.0	21.9	25.3	45.8	62.4	31.4	35.5	42.4	73.7	86.5	110.6	82.5	108.2	86.3	95.6	131.9
9	58.3	42.2	17.7	46.0	3.6	29.1	29.2	20.0	22.8	0.0	20.5	18.0	29.7	60.7	81.4	53.9	54.1	64.8	91.6	106.2	129.4	99.7	129.0	104.6	114.3	150.0
10	69.2	57.1	27.2	62.1	21.4	47.9	46.6	38.1	25.0	20.5	0.0	35.5	11.0	44.1	67.4	47.8	41.5	57.5	76.0	92.3	114.1	83.4	116.2	89.1	99.0	133.9
11	67.3	48.3	33.1	50.0	20.4	30.7	33.5	2.8	21.9	18.0	35.5	0.0	41.6	67.4	84.1	51.2	57.4	62.1	95.6	107.9	132.3	104.4	129.0	108.2	117.3	153.7
12	80.2	68.1	38.2	73.0	31.3	58.2	57.2	44.4	25.3	29.7	11.0	41.6	0.0	33.1	56.6	40.4	31.4	49.0	65.0	81.5	103.0	72.3	105.5	78.0	88.0	122.8
13	113.1	101.0	71.3	105.7	63.1	89.8	89.5	70.2	45.8	60.7	44.1	67.4	33.1	0.0	25.1	32.6	14.6	33.4	32.0	49.2	70.0	39.3	73.8	45.0	55.0	89.8
14	136.5	123.1	94.1	127.3	84.2	110.2	110.5	86.6	62.4	81.4	67.4	84.1	56.6	25.1	0.0	36.4	27.3	29.2	12.7	25.0	48.3	21.9	49.0	24.2	33.2	69.5
15	112.1	95.7	70.0	98.9	57.3	80.2	81.7	53.3	31.4	53.9	47.8	51.2	40.4	32.6	36.4	0.0	18.1	11.0	49.0	57.9	82.9	58.3	77.9	60.2	68.4	104.6
16	110.1	96.0	67.5	100.1	57.0	82.9	83.3	60.0	35.5	54.1	41.5	57.4	31.4	14.6	27.3	18.1	0.0	21.0	38.3	52.1	75.5	47.0	75.2	51.0	60.4	96.6
17	122.9	106.7	80.7	109.9	68.2	91.3	92.8	64.2	42.4	64.8	57.5	62.1	49.0	33.4	29.2	11.0	21.0	0.0	41.9	48.3	73.4	51.0	67.3	51.9	59.4	95.2
18	145.1	132.6	103.1	137.2	94.2	120.6	120.7	98.2	73.7	91.6	76.0	95.6	65.0	32.0	12.7	49.0	38.3	41.9	0.0	18.9	38.1	9.2	43.4	13.0	23.0	58.5
19	161.5	148.0	119.1	152.2	109.1	134.8	135.4	110.4	86.5	106.2	92.3	107.9	81.5	49.2	25.0	57.9	52.1	48.3	18.9	0.0	25.1	18.4	24.7	11.4	12.2	46.9
20	183.1	170.7	141.2	175.1	132.1	158.3	158.5	134.8	110.6	129.4	114.1	132.3	103.0	70.0	48.3	82.9	75.5	73.4	38.1	25.1	0.0	31.3	21.0	25.0	15.1	21.9
21	152.1	140.3	110.5	145.0	102.2	128.8	128.7	107.0	82.5	99.7	83.4	104.4	72.3	39.3	21.9	58.3	47.0	51.0	9.2	18.4	31.3	0.0	40.6	7.8	17.1	50.5
22	185.3	171.1	142.7	175.0	132.1	157.1	158.0	131.2	108.2	129.0	116.2	129.0	105.5	73.8	49.0	77.9	75.2	67.3	43.4	24.7	21.0	40.6	0.0	32.8	24.8	36.5
23	158.1	145.7	116.2	150.2	107.2	133.6	133.7	110.7	86.3	104.6	89.1	108.2	78.0	45.0	24.2	60.2	51.0	51.9	13.0	11.4	25.0	7.8	32.8	0.0	10.0	45.6
24	168.1	155.5	126.1	160.0	117.0	143.2	143.4	119.9	95.6	114.3	99.0	117.3	88.0	55.0	33.2	68.4	60.4	59.4	23.0	12.2	15.1	17.1	24.8	10.0	0.0	36.4
Exit	202.4	190.8	161.0	195.5	152.6	179.1	179.1	156.2	131.9	150.0	133.9	153.7	122.8	89.8	69.5	104.6	96.6	95.2	58.5	46.9	21.9	50.5	36.5	45.6	36.4	0.0

Distance (m)

Table A2
VBA solver stopping criteria and parameter values.

Parameter	Value
Max time	1×10^6
Iterations	1×10^6
Precision	1×10^{-7}
Convergence	1×10^{-2}
Population size	100
Mutation rate	0.9
Max sub-problems	1×10^9
Max time no improvement	1×10^4

Appendix B

(See: Figs. B1–B2)

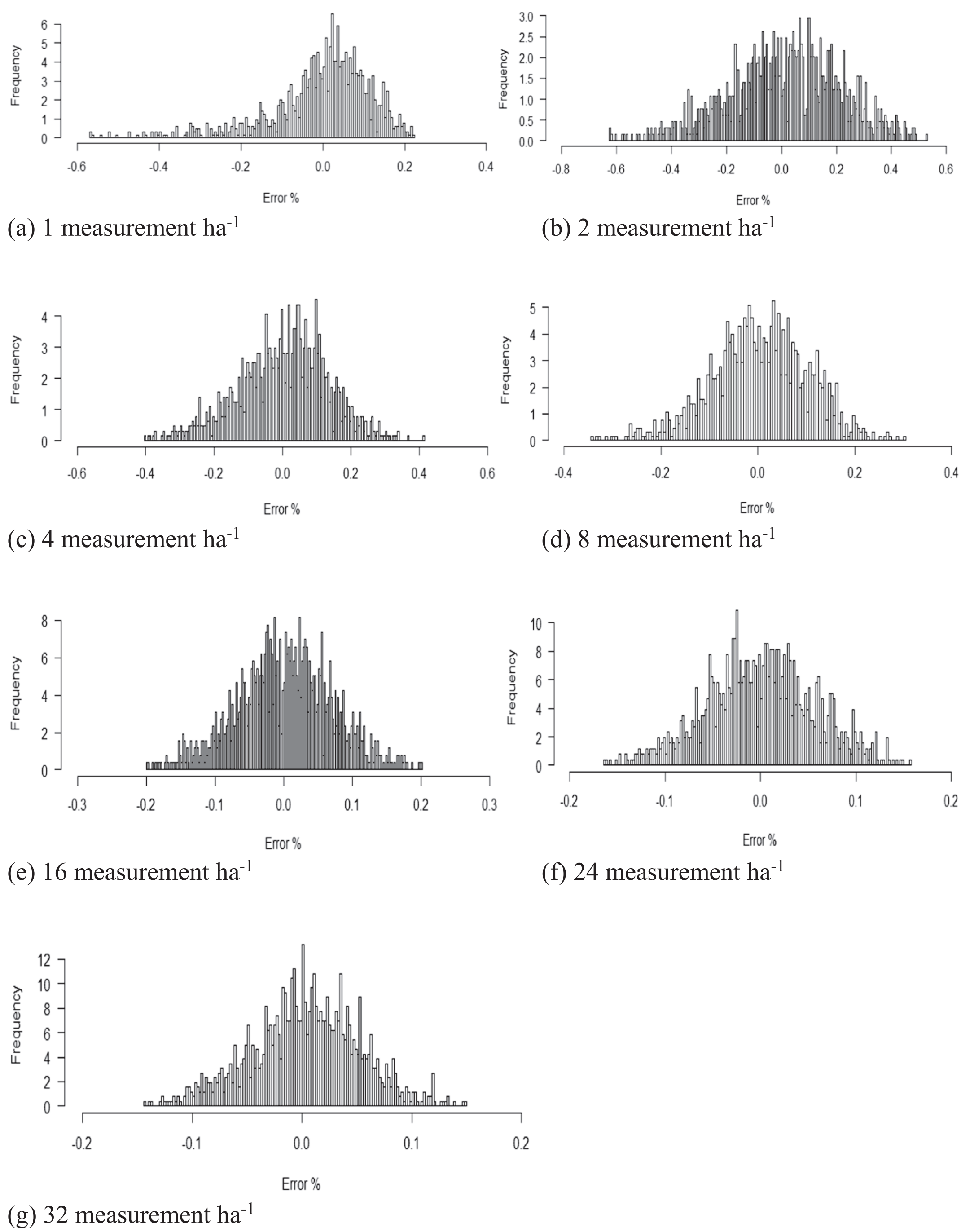

(a) 1 measurement ha^{-1} (b) 2 measurement ha^{-1} (c) 4 measurement ha^{-1} (d) 8 measurement ha^{-1} (e) 16 measurement ha^{-1} (f) 24 measurement ha^{-1} (g) 32 measurement ha^{-1}

Fig. B1. Frequency distribution of estimated compressed sward height measurement error for specified measurement rates.

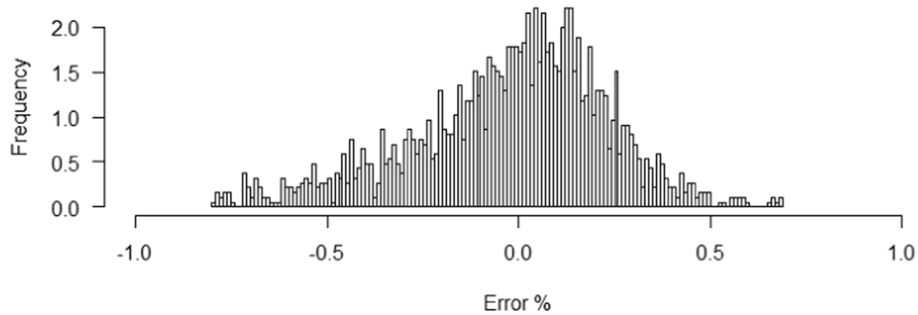

Fig. B2. frequency distribution of monthly herbage mass calibration error across 2017 – 2019 growing seasons.

References

Abdoun, O., Abouchabaka, J., 2012. A comparative study of adaptive crossover operators for genetic algorithms to resolve the traveling salesman problem. Int. J. Comput. Appl. 31, 49–57.

Abdoun, O., Abouchabaka, J., Tajani, C., 2012. Analyzing the performance of mutation operators to solve the travelling salesman problem. Int. J. Emerg. Sci. 2, 61–77.

Ballari, D., de Bruin, S., Bregt, A.K., 2012. Value of information and mobility constraints for sampling with mobile sensors. Comput. Geosci. 49, 102–111. https://doi.org/10.1016/j.cageo.2012.07.005.

Barthram, G.T., Duff, E.I., Elston, D.A., Griffiths, J.H., Common, T.G., Marriott, C.A., 2005. Frequency distributions of sward height under sheep grazing. Grass Forage Sci. 60, 4–16. https://doi.org/10.1111/j.1365-2494.2005.00444.x.

Baudracco, J., Lopez-Villalobos, N., Holmes, C.W., Comeron, E.A., MacDonald, K.A., Barry, T.N., 2013. E-Dairy: A dynamic and stochastic whole-farm model that predicts biophysical and economic performance of grazing dairy systems. Animal 7, 870–878. https://doi.org/10.1017/S1751731112002376.

Beukes, P.C., McCarthy, S., Wims, C.M., Gregorini, P., Romera, A.J., 2019. Regular estimates of herbage mass can improve profitability of pasture-based dairy systems. Anim. Prod. Sci. 59, 359. https://doi.org/10.1071/AN17166.

Cayley, J.W.D., Bird, P.R., 1996. General principles, in: Principles of Environmental Sciences. Victoria. Dept of Agriculture, Energy and Minerals, Hamilton, Australia, pp. 75–83. https://doi.org/10.1007/978-1-4020-9158-2_7.

Delaby, L., Duboc, G., Cloet, E., Martinot, Y., 2015. Pastur'Plan : a dynamic tool to support grazing management decision making in a rotational grazing system, in: van den Pol-van Dasselaar, A., Aarts, H.F.M., Vliegher, A. De, Elgersma, A., Reheul, D., Reijneveld, J.A., Verloop, J., Hopkins, A. (Eds.), Proceedings of the 18th Symposium of the European Grassland Federation. Organising Committee of the 18th Symposium of the European Grassland Federation 2015 and the Nederlandse Vereniging voor Weide- en Voederbouw, Wageningen, NLD, pp. 200–202.

Delaby, L., Peyraud, J.L., Bouttier, A., Peccatte, J.R., 1998. Effet d'une réduction simultanée de la fertilisation azotée et du chargement sur les performances des vaches laitières et la valorisation du pâturage. Anim. Res. 47, 17–39. https://doi.org/10.1051/animres:19980102.

Dillon, P., 2011. The Irish dairy industry-Planning for 2020. In: National Dairy Conference 2011. Cork IRL, pp. 1–24.

Dillon, P., 2006. Achieving high dry-matter intake from pasture with grazing dairy cows. In: Elgersma, A., Dijkstra, J., Tamminga, S. (Eds.), Fresh Herbage for Dairy Cattle: The Key to a Sustainable Food Chain. Springer, New York, USA, pp. 1–26. https://doi.org/10.1007/978-1-4020-5452-5_1.

Earle, D.F., Mc Gowan, A.A., 1979. Evaluation and calibration of an automated rising plate meter for estimating dry matter yield of pasture. Aust. J. Exp. Agric. 19, 337–343. https://doi.org/10.1071/EA9790337.

Ferraro, F.P., Nave, R.L.G., Sulc, R.M., Barker, D.J., 2012. Seasonal variation in the rising plate meter calibration for forage mass. Agron. J. 104, 1–6. https://doi.org/10.2134/agronj2011.0190.

Fylstra, D., Lasdon, L., Watson, J., Waren, A., 1998. Design and use of the Microsoft Excel Solver. Interf. 28, 29–55. https://doi.org/10.1287/inte.28.5.29.

Grafton, M., Manning, M., 2017. Establishing a risk profile for New Zealand pastoral farms. Agric. 7 https://doi.org/10.3390/agriculture7100081.

Hanrahan, L., Geoghegan, A., O'Donovan, M., Griffith, V., Ruelle, E., Wallace, M., Shalloo, L., 2017. PastureBase Ireland: A grassland decision support system and national database. Comput. Electron. Agric. 136, 193–201. https://doi.org/10.1016/j.compag.2017.01.029.

Hanrahan, L., McHugh, N., Hennessy, T., Moran, B., Kearney, R., Wallace, M., Shalloo, L., 2018. Factors associated with profitability in pasture-based systems of milk production. J. Dairy Sci. 101, 5474–5485. https://doi.org/10.3168/jds.2017-13223.

Haupt, R., Haupt, S., 2004. Advanced Applications. In: Practical Genetic Algorithms. John Wiley & Sons Inc, Hoboken, pp. 151–184.

Haydock, K.P., Shaw, N.H., 1975. The comparative yield method for estimating dry matter yield of pasture. Aust. J. Exp. Agric. 15, 663–670. https://doi.org/10.1071/EA9750663.

Hirata, M., 2000. Quantifying spatial heterogeneity in herbage mass and consumption in pastures. J. Range Manag. 53 https://doi.org/10.2458/azu_jrm_v53i3_hirata.

Holshof, G., Stienezen, M., Galama, P., 2015. Calibration of five rising plate meters in the Netherlands. In: van den Pol-van Dasselaar, A., Aarts, H.F.M., Vliegher, A. De, Elgersma, A., Reheul, D., Reijneveld, J.A., Verloop, J., Hopkins, A. (Eds.), Grassland and Forages in High Output Dairy Farming Systems. Wageningen Academic Publishers, Wageningen, The Netherlands, pp. 233–235.

Hutchinson, K.J., Scobie, D.R., Beautrais, J., Mackay, A.D., Rennie, G.M., Moss, R.A., Dynes, R.A., 2016. A protocol for sampling pastures in hill country. J. New Zeal. Grasslands 78, 203–210.

Jiang, C., 2010. A reliable solver of euclidean traveling salesman problems with microsoft excel add-in tools for small-size systems. J. Softw. 5, 761–768. https://doi.org/10.4304/jsw.5.7.761-768.

Jordan, C., Shi, Z., Bailey, J.S., Higgins, A.J., 2003. Sampling strategies for mapping "within-field" variability in the dry matter yield and mineral nutrient status of forage grass crops in cool temperate climes. Precis. Agric. 4, 69–86. https://doi.org/10.1023/A:1021815122216.

Keller, J.M., Liu, D., Fogel, D.B., 2016. Fundamentals of Computational Intelligence: Neural Networks, Fuzzy Systems, and Evolutionary Computation. John Wiley & Sons Inc, New Jersey, USA, 10.1002/9781119214403.

Klootwijk, C.W., Holshof, G., de Boer, I.J., Van den Pol-Van Dasselaar, A., Engel, B., Van Middelaar, C.E., 2019a. Correcting fresh grass allowance for rejected patches due to excreta in intensive grazing systems for dairy cows. J. Dairy Sci. 102, 10451–10459. https://doi.org/10.3168/jds.2018-16120.

Klootwijk, C.W., Holshof, G., van den Pol-van Dasselaar, A., van Helvoort, K.L.M., Engel, B., de Boer, I.J.M., van Middelaar, C.E., 2019b. The effect of intensive grazing systems on the rising plate meter calibration for perennial ryegrass pastures. J. Dairy Sci. 102, 10439–10450. https://doi.org/10.3168/jds.2018-16118.

Lile, J.A., Blackwell, M.B., Thomson, N.A., Penno, J.W., Macdonald, K.A., Nicholas, P.K., Lancaster, J.A.S., Coulter, M., 2001. Practical use of the rising plate meter (RPM) on New Zealand dairy farms. J. New Zeal. Grasslands 63, 159–164.

Maher, J., Bogue, F., Douglas, J., 2019. Grass10 campaign. In: Moorepark '19 Irish Dairying – Growing Sustainably. Teagasc, Moorepark, Fermoy, Ireland, pp. 62–64.

Manderson, A., Hunt, C., 2013. Introducing the Agri-Rover: An Autonomous on-the-go sensing rover for science and farming, in: Currie, L., Christensen, C.L. (Eds.), Proceedings of the 26th Annual FLRC Workshop Held at Massey University. Massey University, Palmerston North, New Zealand.

Mannetje, L.T., 2000. Measuring biomass of grassland Vegetation. In: Mannetje, L.T., Jones, R.M. (Eds.), Field and Laboratory Methods for Grassland and Animal Production Research. CABI Publishing, Oxon, UK, pp. 151–178.

McSweeney, D., Coughlan, N.E., Cuthbert, R.N., Halton, P., Ivanov, S., 2019. Micro-sonic sensor technology enables enhanced grass height measurement by a Rising Plate Meter. Inf. Process. Agric. 6, 279–284. https://doi.org/10.1016/j.inpa.2018.08.009.

Microsoft, 2020. SolverOptions Function | Microsoft Docs [WWW Document]. URL https://docs.microsoft.com/en-us/office/vba/excel/concepts/functions/solveroptions-function (accessed 4.24.20).

Microsoft, 2010. Visual Basics for Applications 7 [WWW Document]. URL https://www.microsoft.com/en-ie/microsoft-365/p/excel (accessed 10.10.17).

Minetti, A., 2000. The three modes of terrestrial locomotion. In: Nigg, B.M., MacIntosh, B.R., Mester, J. (Eds.), Biomechanics and Biology of Movement. Human Kinetics, Champaign, IL, USA, pp. 67–78.

Murphy, D.J., O' Brien, B., Askari, M.S., McCarthy, T., Magee, A., Burke, R., Murphy, M. D., 2019a. GrassQ - a holistic precision grass measurement and analysis system to optimize pasture based livestock production, in: ASABE Annual Interantional Meeting. American Society of Agricultural and Biological Engineers, St. Joseph, MI, USA, pp. 2–9. https://doi.org/10.13031/aim.201900769.

Murphy, D.J., O' Brien, B., Hennessy, D., Hurley, M., Murphy, M.D., 2020a. Evaluation of the precision of the rising plate meter for measuring compressed sward height on heterogeneous grassland swards. Under Review.

Murphy, D.J., O' Brien, B., Murphy, M.D., 2018. Development of a labour utilisation decision support tool to efficiently measure grass herbage mass using a rising plate meter, in: ASABE Annual Interantional Meeting. American Society of Agricultural and Biological Engineers, St. Joseph, MI, USA. https://doi.org/10.13031/aim.201800806.

Murphy, D.J., Shine, P., O' Brien, B., O'Donovan, M., Murphy, M.D., 2020b. Utilising grassland management and climate data for more accurate prediction of herbage mass using the rising plate meter. Under Review.

Nakagami, K., 2016. A method for approximate on-farm estimation of herbage mass by using two assessments per pasture. Grass Forage Sci. 71, 490–496. https://doi.org/10.1111/gfs.12195.

O' Leary, M., O' Donovan, M., 2019. PastureBase Ireland — getting Ireland utilising more grass, in: Moorepark '19 Irish Dairying – Growing Sustainably. Teagasc, Moorepark, pp. 60–61.

OSI, 2008. Project planning for the transformation of geographic data from Irish Grid (IG) to Irish Transverse Mercator (ITM). Ordnance Survey Ireland.
O' Sullivan, M., O'keeffe, W.F., Flynn, M.J., 1987. The value of pasture height in the measurement of dry matter yield. Irish J. Agric. Res. 26, 63–68.
Patterson, M.C., Harmel, B., 2003. An algorithm for using Excel Solver© for the traveling salesman problem. J. Educ. Bus. 78, 341–346. https://doi.org/10.1080/08832320309598624.
Rasmussen, R., 2011. TSP in spreadsheets - a guided tour. Int. Rev. Econ. Educ. 10, 94–116. https://doi.org/10.1016/S1477-3880(15)30037-2.
Rayburn, E.B., Shockey, W.L., Seymour, D.A., Smith, B.D., Basden, T.J., 2017. Calibration of pasture forage mass to plate meter compressed height is a second-order response with a zero intercept. Crop. Forage Turfgrass Manag. 3 https://doi.org/10.2134/cftm2017.01.0003.
Reidy, K., 1988. Risk analysis in agricultural development projects: the use of the monte-carlo simulation technique. Irish J. Agric. Econ. Rural Sociol. 13, 35–46.
Rexhepi, A., Maxhuni, A., Dika, A., 2013. Analysis of the impact of parameters values on the Genetic Algorithm for TSP. Int. J. Comput. Sci. 10, 158–164.
Romera, A.J., Beukes, P., Clark, C., Clark, D., Levy, H., Tait, A., 2010. Use of a pasture growth model to estimate herbage mass at a paddock scale and assist management on dairy farms. Comput. Electron. Agric. 74, 66–72. https://doi.org/10.1016/j.compag.2010.06.006.
Sanderson, M.A., Rotz, C.A., Fultz, S.W., Rayburn, E.B., 2001. Estimating forage mass with a commercial capacitance meter, rising plate meter, and pasture ruler. Agron. J. 93, 1281–1286. https://doi.org/10.2134/agronj2001.1281.
Sathyan, A., Boone, N., Cohen, K., 2015. Comparison of approximate approaches to solving the travelling salesman problem and its application to UAV swarming. Int. J. Unmanned Syst. Eng. 3, 1–16. https://doi.org/10.14323/ijuseng.2015.1.
Shalloo, L., Dillon, P., Rath, M., Wallace, M., 2004. Description and validation of the moorepark dairy system model. J. Dairy Sci. 87, 1945–1959. https://doi.org/10.3168/jds.S0022-0302(04)73353-6.
Shalloo, L., Donovan, M.O., Leso, L., Werner, J., Ruelle, E., Geoghegan, A., Delaby, L., Leary, N.O., 2018. Review: Grass-based dairy systems, data and precision technologies. Animal. https://doi.org/10.1017/S175173111800246X.
Stevens, D.L., Olsen, A.R., 2004. Spatially balanced sampling of natural resources. J. Am. Stat. Assoc. 99, 262–278. https://doi.org/10.1198/016214504000000250.
Stray, B.J., van Vuuren, J.H., Bezuidenhout, C.N., 2012. An optimisation-based seasonal sugarcane harvest scheduling decision support system for commercial growers in South Africa. Comput. Electron. Agric. 83, 21–31. https://doi.org/10.1016/j.compag.2012.01.009.
Teagasc, 2018. Teagasc National Farm Survey 2018 - Dairy Enterprise Factsheet [WWW Document]. URL https://www.teagasc.ie/publications/2019/teagasc-national-farm-survey-2018-results.php (accessed 4.23.20).
Thomson, N.A., 1983. Factors influencing the accuracy of herbage mass determinations with a capacitance meter. New Zeal. J. Exp. Agric. 11, 171–176. https://doi.org/10.1080/03015521.1983.10427749.
Thomson, N.A., Mccallum, D.A., Howse, S., Holmes, C.W., Matthews, P.N.P., Matthew, C., 1997. Estimation of dairy pastures - the need for standardisation. J. New Zeal. Grasslands 59, 221–225.
Webster, R., Lark, R.M., 2012. Field Sampling for Environmental Science and Management. Routledge, Oxon, UK.
Xiong, Y., Ge, Y., Liang, Y., Blackmore, S., 2017. Development of a prototype robot and fast path-planning algorithm for static laser weeding. Comput. Electron. Agric. 142, 494–503. https://doi.org/10.1016/j.compag.2017.11.023.
Zhou, K., Leck Jensen, A., Sørensen, C.G., Busato, P., Bothtis, D.D., 2014. Agricultural operations planning in fields with multiple obstacle areas. Comput. Electron. Agric. 109, 12–22. https://doi.org/10.1016/j.compag.2014.08.013.
Zom, R.L.G., Holshof, G., 2011. GrazeVision: A versatile grazing decision support model. In: Pötsch, E.M., Krautzer, B., Hopkins, A. (Eds.), Proceedings of the 16th Symposium of the European Grassland Federation. Organising Committee of the 16th Symposium of the European Grassland Federation 2011 and Agricultural Research and Education Centre. Raumberg-Gumpenstein, Austria, pp. 226–228.